Releasable Layer-by-Layer Assembly of Stabilized Lipid Nanocapsules on Microneedles for Enhanced Transcutaneous Vaccine Delivery

Peter C. DeMuth,[†,#] James J. Moon,[†,‡,#] Heikyung Suh,[†,‡,▽] Paula T. Hammond,[§,⊥,∥,*] and Darrell J. Irvine[†,‡,⊥,∥,△,▽]

[†]Department of Biological Engineering, [‡]Department of Materials Science and Engineering, [§]Department of Chemical Engineering, [⊥]Koch Institute for Integrative Cancer Research, and [∥]Institute for Soldier Nanotechnologies, Massachusetts Institute of Technology, 77 Massachusetts Avenue, Cambridge, Massachusetts 02139, United States, [△]Ragon Institute of MIT, MGH, and Harvard, Boston, Massachusetts 02114, United States, and [▽]Institute for Soldier Nanotechnologies, Howard Hughes Medical Institute, 4000 Jones Bridge Road, Chevy Chase, Maryland 20815, United States. [#]These authors contributed equally to this work.

ABSTRACT Here we introduce a new approach for transcutaneous drug delivery, using microneedles coated with stabilized lipid nanocapsules, for delivery of a model vaccine formulation. Poly(lactide-*co*-glycolide) microneedle arrays were coated with multilayer films *via* layer-by-layer assembly of a biodegradable cationic poly(β-amino ester) (PBAE) and negatively charged interbilayer-cross-linked multilamellar lipid vesicles (ICMVs). To test the potential of these nanocapsule-coated microneedles for vaccine delivery, we loaded ICMVs with a protein antigen and the molecular adjuvant monophosphoryl lipid A. Following application of microneedle arrays to the skin of mice for 5 min, (PBAE/ICMV) films were rapidly transferred from microneedle surfaces into the cutaneous tissue and remained in the skin following removal of the microneedle arrays. Multilayer films implanted in the skin dispersed ICMV cargos in the treated tissue over the course of 24 h *in vivo*, allowing for uptake of the lipid nanocapsules by antigen presenting cells in the local tissue and triggering their activation *in situ*. Microneedle-mediated transcutaneous vaccination with ICMV-carrying multilayers promoted robust antigen-specific humoral immune responses with a balanced generation of multiple IgG isotypes, whereas bolus delivery of soluble or vesicle-loaded antigen *via* intradermal injection or transcutaneous vaccination with microneedles encapsulating soluble protein elicited weak, IgG_1-biased humoral immune responses. These results highlight the potential of lipid nanocapsules delivered by microneedles as a promising platform for noninvasive vaccine delivery applications.

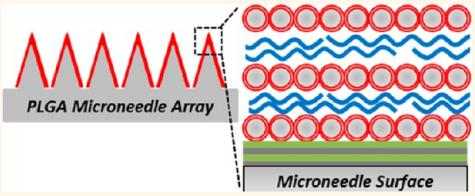

KEYWORDS: layer-by-layer · transcutaneous delivery · microneedles · vaccine · polymer assembly · biodegradable

The generation of polyelectrolyte multilayers (PEMs) through the iterative and sequential adsorption of complementary materials is an attractive approach for nanoscale assembly of functional systems capable of controlled encapsulation and delivery of diverse therapeutics. The inherent adaptability of multilayer processing, as well as its biocompatibility, scalability, and simplicity, makes it an ideal strategy for the creation of conformal coatings on complex surfaces (reviewed in refs 1, 2). Recently, multilayers have been optimized for the encapsulation of lipid vesicles, with the aim of increasing the drug loading capacity of multilayer films, allowing for biological cargos to be entrapped in films in native aqueous conditions, and providing triggered materials release through programmed vesicle disruption.[3−10] A key issue for incorporation of liposomal carriers in multilayer films is the need for stabilization of vesicles against rupture during the assembly process or drying of the resulting films. Previous approaches have relied on vesicle stabilization strategies such as *in situ* silica polymerization[3,4] or polyelectrolyte adsorption on the vesicle surface prior to multilayer assembly.[5−10] Without such stabilizing measures, layer-by-layer (LbL) deposition results in spontaneous vesicle disruption into lipid bilayers on the target substrate.

We recently reported a new approach for lipid vesicle stabilization, where covalent cross-links are introduced between adjacent phospholipid bilayers in the walls of multilamellar vesicles to create robust lipid nanocapsules.[11,12] These interbilayer-cross-linked multilamellar vesicles (ICMVs) encapsulate protein cargos within their interior and exhibit enhanced serum stability in extracellular conditions, but can be readily degraded upon cellular internalization.[11] Vaccination with ICMVs elicited potent cellular and humoral immune responses against the model antigen ovalbumin (OVA) and enhanced long-term humoral responses to a

* Address correspondence to hammond@mit.edu, djirvine@mit.edu.

Received for review June 14, 2012 and accepted August 24, 2012.

Published online August 24, 2012
10.1021/nn302639r

recombinant malaria antigen following subcutaneous injection.[11,12] Given their enhanced stability and unique potency in the context of protein vaccine delivery, we hypothesized that LbL deposition of ICMVs would provide an interesting opportunity for the design of ICMV-containing multilayer delivery systems for subunit vaccination.

In parallel studies, we and others have recently demonstrated the utility of microneedle arrays for the safe, rapid, and convenient delivery of drugs through the pain-free disruption of the stratum corneum to access the immune-competent epidermal and dermal tissue.[13−15] Microneedles have particularly shown promise in vaccine delivery.[15−17] Microneedle application is known to improve safety, eliminate pain upon treatment, and reduce the generation of hazardous medical waste associated with needle-based delivery.[18−20] Further, creation of conformal surface coatings on microneedle arrays has proven to be an effective method for therapeutic formulation and delivery into the skin *via* rapid, topical microneedle application.[15,21] We therefore set out to design a PEM system for the stable encapsulation and release of ICMVs for transcutaneous delivery into the skin *via* microneedle insertion. We envisioned several potential advantages for such an approach including (i) improved dry state storage through PEM-embedding of ICMVs, (ii) controlled encapsulation and release of ICMVs from degradable PEMs implanted in the skin, (iii) delivery of ICMVs to an inherently immunogenic tissue for enhanced immunity through microneedle application, and (iv) convenient and self-contained combination of vaccine and administration device for rapid, safe, and painless vaccine delivery that could potentially be self-administered in minutes.

Here we report studies intended to test these hypotheses, focusing on the generation of a PEM system capable of stable ICMV encapsulation and release for protein immunization. We first show the ability of degradable PEMs to stably incorporate ICMV particles, on both flat silicon substrates and poly(lactide-coglycolide) (PLGA) microneedles, controlling film thickness and ICMV dosage and verifying that incorporated ICMVs are intact within dried multilayer films. We then demonstrate the ability for PEM-coated microneedles to transfer their ICMV-loaded films into the cutaneous tissue upon brief application to the skin of mice. Following film degradation and ICMV dispersion in the epidermal tissue, ICMVs were found to be taken up by resident antigen presenting cells (APCs) within the skin, which were activated *in situ* by adjuvants delivered by the particles. Finally, we show that transcutaneous vaccination with ICMVs embedded in microneedle-based multilayers significantly enhanced humoral immune responses to a protein antigen, compared to mice vaccinated with either conventional intradermal bolus injection of antigen or microneedle-mediated delivery of soluble protein antigen. Together, these results suggest the potential of microneedle-based multilayers for the effective transcutaneous delivery of functional nanoscale vesicles. In this work, we have improved protein subunit vaccination by taking advantage of the immunogenicity of ICMVs delivered to the skin, a site known for high frequency of epidermal and dermal APCs; however, this work describing vesicle deposition on multilayer-coated microneedles can be readily adapted as a modular, general strategy for noninvasive drug delivery to the skin.

RESULTS AND DISCUSSION

We recently demonstrated that microneedles coated with PLGA nanoparticle-loaded PEMs could be used for rapid implantation of particle-loaded films in skin.[15] PLGA particles are attractive for small-molecule drug delivery but have limitations for delivery of biologics such as vaccines, due to the low doses of proteins that can be encapsulated and the potential for antigen denaturation during processing. We hypothesized that the deposition of an ICMV-containing multilayer coating on the surface of microneedles would provide a solution to these issues and enable a simple, self-contained, and effective method for recombinant protein vaccine storage and delivery to the skin, an attractive tissue target due to its dense matrix of resident innate immune cells (Figure 1).[22−24] To fabricate an erodible PEM system capable of encapsulating and delivering intact nanoscale vesicles, we selected Poly-1 (Figure S1), a biocompatible, hydrolytically degradable polymer from a class of polyelectrolytes known as poly(β-amino esters) (PBAEs), to serve as a complementary degradable partner for ICMV encapsulation in multilayers. Poly-1 has been extensively studied in a variety of contexts and has been proven effective in generating erodible multilayer films containing many diverse cargos for controlled drug release.[15,21,25−29] We selected ICMVs to serve as a stable polyanionic vesicular partner for Poly-1 in multilayer deposition, taking advantage of their colloidal stability and potency as vaccine delivery vehicles.[11,12] In this context, ICMVs could serve as a modular delivery vehicle for antigen and adjuvant incorporated in either the aqueous vesicle core or the hydrophobic lipid capsule walls of ICMVs, and the covalent interbilayer maleimide cross-links would provide stability for multilayer encapsulation (Figure 1a). We hypothesized that (Poly-1/ICMV) multilayers would be deposited into the skin through brief topical microneedle application (Figure 1b), where hydrolytic degradation of Poly-1 over time would lead to ICMV release (Figure 1c) into the surrounding tissue, followed by uptake into local APCs (Figure 1d) that would initiate adaptive immunity.

Negatively charged ICMVs encapsulating fluorescent OVA and composed of DOPC and maleimide-lipid MPB (Figure S1) in a 1:1 mol ratio (diameter 240 $\pm$ 10 nm, 0.19 $\pm$ 0.05 polydispersity index, zeta potential

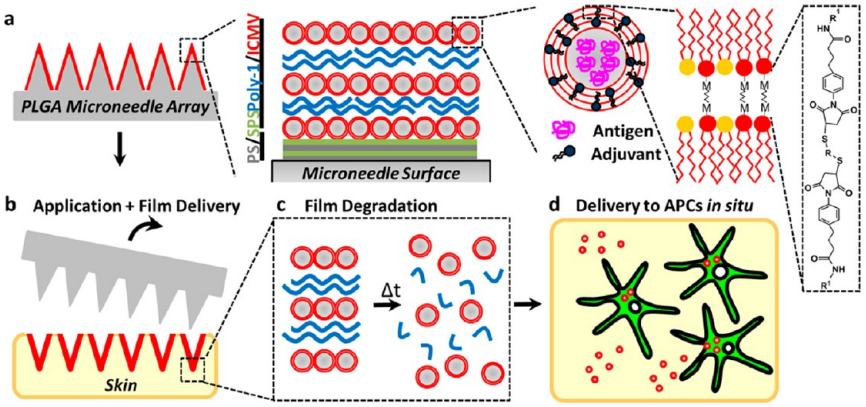

Figure 1. (a) Schematic illustration of (Poly-1/ICMV) multilayers deposited onto PLGA microneedle surfaces. ICMV lipid nanocapsules are prepared with interbilayer covalent cross-links between maleimide head groups (M) of adjacent phospholipid lamellae in the walls of multilamellar vesicles. (Poly-1/ICMV) PEMs were constructed on microneedles after (PS/SPS) base layer deposition. (b) Microneedles transfer (Poly-1/ICMV) coatings into the skin as cutaneous depots at microneedle insertion points. (c) Hydrolytic degradation of Poly-1 leads to PEM disintegration and ICMV release into the surrounding tissue. (d) ICMV delivery to skin-resident APCs provides coincident antigen exposure and immunostimulation, leading to initiation of adaptive immunity.

-41 ± 1.0 mV, incorporating 0.1 wt % DiI as a fluorescent tracer in the vesicle walls) were prepared as previously described.[11,12] To determine whether ICMVs could be stably embedded into degradable multilayer films, we first synthesized model LbL films on atomically flat silicon substrates. First, 20 bilayers of protamine sulfate (PS) and sulfonated poly(styrene) (SPS) were deposited to form a base layer of uniform surface charge.[15,30] Through subsequent LbL steps, we attempted to construct ICMV-encapsulating multilayers through sequential immersion in aqueous Poly-1 and ICMV suspensions of varying concentrations. As shown in Figure 2a, when LbL assembly was performed using ICMVs at 0.5 mg/mL in phosphate-buffered saline (PBS) at pH 5.0, we observed insignificant and irregular film growth, with film thickness remaining steady after 15 deposition cycles at ~400 nm as measured by profilometry. However, using a more concentrated 1 mg/mL ICMV dispersion, we observed a regular linear increase in measured film thickness (~50 nm/bilayer) with each deposition cycle up to 35 rounds of LbL deposition, resulting in films more than 1.5 μm thick (Figure 2a). For comparison with the cross-link-stabilized ICMVs, we also synthesized non-cross-linked multilamellar vesicles (MLVs) *via* the same process used to prepare ICMVs, leaving out the final interbilayer cross-linking step. In contrast to ICMVs, MLVs (diameter 270 ± 17 nm, 0.23 ± 0.014 polydispersity index, zeta potential -33.6 ± 0.9 mV) displayed inconsistent and irregular film growth, plateauing at ~500 nm after 15 bilayers (Figure 2a). This result is consistent with previous evidence showing ineffective LbL growth of phospholipid vesicles without sufficient stabilization to prevent spontaneous disruption upon adsorption.[31,32] Spectroscopic measurement of fluorescent signal obtained after (Poly-1/ICMV) film disruption in NaCl for 24 h indicated a loading of ~5 μg OVA/cm^2 and ~15 μg lipids/cm^2 for multilayers containing 35 bilayers (~1.6 μm in thickness), consistent with the known OVA loading density of intact ICMVs;[11] this loading is within the effective dose range needed for ICMVs to generate potent immune responses *in vivo* when administered by traditional routes.[11,12] Further, previous studies have demonstrated enhanced potency of transcutaneously administered vaccines, suggesting that additional dose sparing might be possible in this context.[33−35]

Given the success of film growth at these initial conditions, we then measured the effect of deposition time on the growth of (Poly-1/ICMV)-containing films and observed no significant increase in film growth per bilayer when the duration for Poly-1 and ICMV adsorption was increased from 5 to 10 min (Figure 2b). We thus concluded that 5 min was a sufficient time period to achieve ICMV adsorption and reversal of surface charge for successful LbL adsorption. To confirm that ICMVs were stably incorporated into Poly-1 films, we performed confocal laser scanning microscopy (CLSM) on (Poly-1/ICMV) multilayers constructed using ICMVs labeled with DiI in the lipid phase of the particles and encapsulating fluorescent AF647-OVA. CLSM imaging showed the presence of overlaid punctate fluorescent signals indicating co-localization of AF647-OVA and DiI in submicrometer spherical particles, suggesting the incorporation of intact, OVA-loaded ICMVs into Poly-1 multilayers (Figure 2c). This punctate fluorescent signal was not observed in films constructed using MLVs formed in the absence of interbilayer cross-links, and only low levels of OVA fluorescence were detected in such films, providing evidence for the importance of the stabilizing interbilayer cross-links of ICMVs for preventing vesicle disruption during LbL processing (Figure 2c). In addition, large contiguous patches of the DiI lipid tracer were observed in films prepared with non-cross-linked MLVs, suggesting fusion among

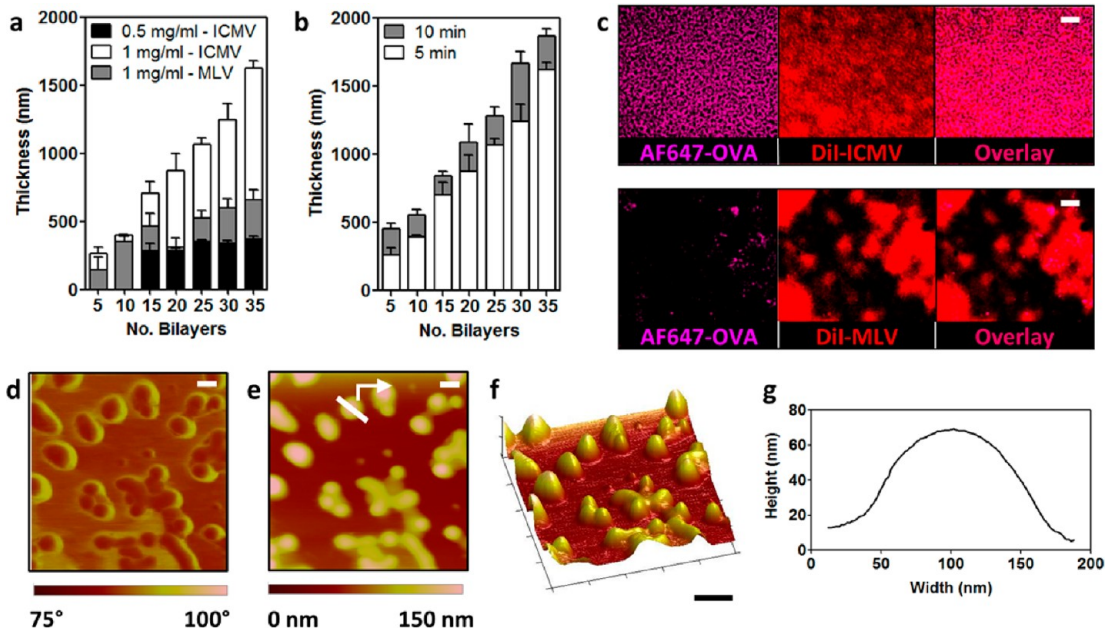

Figure 2. Shown are Poly-1/lipid film thicknesses determined by profilometry for deposited ICMVs or MLVs varying (a) concentration and (b) deposition time (n = 12). (c) CLSM image of $(PS/SPS)_{20}(Poly\text{-}1/ICMV)_{20}$ or $(PS/SPS)_{20}(Poly\text{-}1/MLV)_{20}$ multilayers deposited on silicon (scale bar ~20 μm). ICMVs and MLVs contained AF647-OVA (pink) and were labeled with DiI (red). (d–g) AFM imaging of a dried $(Poly\text{-}1/ICMV)_5(PS/SPS)_{20}$ multilayer built on silicon (scale bar 100 nm). Shown are (d) phase, (e) height, and (f) 3-D rendered AFM height micrograph data for a $(Poly\text{-}1/ICMV)_5(PS/SPS)_{20}$ multilayer (scale bar 100 nm). (g) Height trace data (trace shown in panel (e) for a single embedded ICMV in a $(PS/SPS)_{20}(Poly\text{-}1/ICMV)_5$ multilayer).

vesicles occurring in this case (Figure 2c). To obtain further confirmation of intact ICMV incorporation into multilayers, we performed atomic force microscopy (AFM) to investigate the surface of (Poly-1/ICMV) films on silicon. Consistent with previous studies showing intact vesicle incorporation,[3,4,8–10] we observed individual spherical structures 100–300 nm in diameter in height and phase AFM images, suggesting that multilayer-embedded ICMVs were intact and unchanged following LbL deposition (Figure 2d, e). This was readily apparent upon 3-D rendering of AFM height data (Figure 2f) and in analysis of height traces (Figure 2g), suggesting individual ICMVs embedded within the (Poly-1/ICMV) multilayers. The exposed dimensions of particles at the top of films measured in this way showed diameters of ~100–300 nm and heights of ~50–75 nm, consistent with the previously measured average bilayer thickness and suggesting some deformation and burial of the particles in underlying Poly-1 layers, as observed in prior studies of vesicles incorporated in multilayers.[6,9] Additional AFM measurement of dry films stored at room temperature for 7 days revealed similar punctate patterns with no significant change in dimension, indicating the potential for multilayer encapsulated ICMVs to maintain their structure upon dry-state storage (Figure S2), an attractive feature for potential vaccine delivery systems in the developing world.

Given the ability of Poly-1 multilayers to encapsulate intact ICMVs, we next sought to use this approach for ICMV delivery and release into the skin. We and others have recently reported the successful generation of multilayer films on the surface of microneedle arrays for transcutaneous delivery *in vivo*.[15,21] We hypothesized that a similar approach could allow for ICMV-loaded multilayer delivery, and given the demonstrated potency of ICMVs for generating adaptive immunity,[11,12] we anticipated that ICMV delivery to the APC-rich epidermis might provide enhanced dose sparing immunogenicity. To test whether ICMV-loaded multilayers could be deposited as surface coatings on microneedles, we first fabricated PLGA microneedles using poly(dimethyl siloxane) (PDMS) molding as previously described,[15] yielding arrays of conical microneedles each ~650 μm in height and 250 μm in diameter at the base. Then, following (PS/SPS) baselayer deposition on these microneedles, we performed LbL assembly using fluorescently labeled DiI-ICMVs encapsulating AF647-OVA as before. CLSM on the resulting multilayer-coated microneedles revealed consistent and uniform fluorescent signal localized to the surface of each microneedle, indicating effective multilayer deposition as observed for flat silicon substrates (Figure 3a). Using confocal z-scanning, we then performed quantitative analysis of the total fluorescent signal on individual microneedles following deposition of 10, 20, or 30 bilayers. This analysis demonstrated a similar linear growth profile for both DiI-labeled ICMVs and the encapsulated AF647-OVA cargo, consistent with the thickness increase measured with profilometry on silicon (Figure 3b). In addition to confirming the similar growth of silicon- and microneedle-based films,

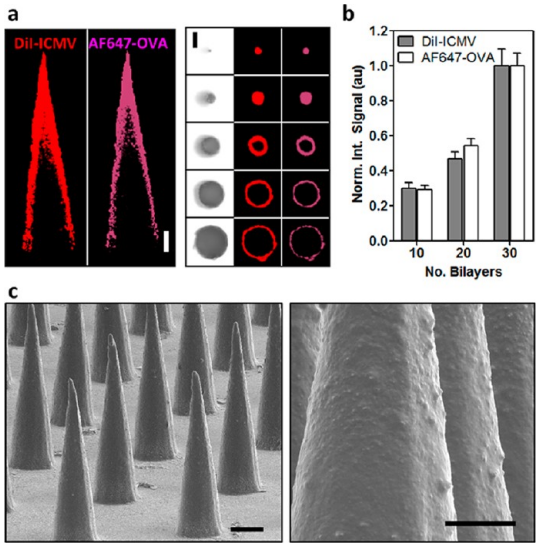

Figure 3. (a) Representative confocal images of PLGA microneedles coated with $(PS/SPS)_{20}(Poly\text{-}1/ICMV)_{35}$ films (left, transverse optical sections; right, lateral sections; 100 μm interval; scale bar 100 μm; red, DiI-ICMVs; pink, AF647-OVA). (b) Quantification of DiI-ICMV and AF647-OVA incorporation into $(PS/SPS)_{20}(Poly\text{-}1/ICMV)_n$ films on microneedles. Analysis was performed using ImageJ measurement of total fluorescent signal intensity in confocal *z*-stacks collected along the length of microneedles, normalized to the total intensity obtained for 30 bilayer films (results shown are averaged from $n = 15$ individual microneedles per condition). (c) SEM micrographs of $(PS/SPS)_{20}(Poly\text{-}1/ICMV)_{35}$ multilayer-coated PLGA microneedles (scale bars: left 200 μm, right 50 μm).

these results provide additional evidence for intact ICMV incorporation on microneedle surfaces, consistent with our previous demonstration of nanoparticle encapsulation on microneedle arrays through spray LbL deposition.[15] Finally, we imaged the resulting multilayer-coated microneedles using scanning electron microscopy (SEM) and observed the presence of consistent surface coatings uniformly covering the entire microneedle array surface (Figure 3c).

We next tested whether microneedle-based multilayers encapsulating ICMVs were delivered into skin following microneedle application *in vivo*. We have previously shown that microneedles similar to those used here are effective in providing consistent disruption of the stratum corneum and insertion into the outer layers of the skin following brief topical application to the skin of mice.[15] We confirmed this result using trypan blue staining of treated skin and observed uniform staining patterns indicating microneedle insertion as before (data not shown). To test for transcutaneous delivery, multilayer-coated microneedles carrying AF647-OVA-loaded, DiI-labeled ICMVs were applied to the dorsal ear or flank skin of C57Bl/6 mice. We then performed quantitative CLSM image analysis to determine the relative loss of fluorescent signal from individual microneedles following application. Microneedles applied for only 5 min showed significant losses of both DiI and AF647-OVA fluorescent signal over the entire microneedle surface, with ~80% reduction in fluorescent intensity observed on the microneedle surfaces (Figure 4a–c). Fluorescent signal reduction was equivalent for both the lipophilic tracer and protein cargo, suggesting delivery of intact multilayer-embedded ICMVs. These results are consistent with our previous demonstration of polymer nanoparticle-loaded multilayer delivery, in which we observed that, unlike multilayers composed only of polymeric materials, PEMs containing embedded particles were rapidly transferred to the skin after brief application of microneedle arrays.[15] This difference in the kinetics of multilayer transfer may reflect a decreased degree of interpenetrating molecular entanglements between complementary polymer and nanoparticle pairs, compared to multilayers composed of complementary polymers alone. The microneedles themselves make up 45% of the total coated surface area on the microneedle array, meaning that with 80% delivery of the coated material, overall ~36% of the vaccine components coated on the microneedles are estimated to be delivered into the skin. Approaches to increase this fraction can be readily envisioned by using a hydrophobic base to prevent wetting of the backing and/or employing strategies to carry out LbL deposition only on the microneedle tips.[21,36]

We next examined microneedle-treated skin to observe deposition of ICMV-loaded multilayers into the tissue. ICMVs were prepared with AF647-OVA loaded in the aqueous core as a model protein antigen. As adjuvants to provide local inflammatory cues necessary to drive the immune response, we embedded the Toll-like receptor (TLR)-4 agonist monophosphoryl lipid A (MPLA) in the ICMV capsule walls and further applied aqueous solutions of the TLR-3 agonist polyI:C (a double-stranded RNA mimic of viral RNA) directly to the skin just prior to microneedle application. To observe ICMV delivery in relation to target APC populations in the skin, we applied microneedles to the skin of MHC II-GFP mice. These animals express all major histocompatibility class II (MHC II) molecules as a fusion with green fluorescent protein (GFP), allowing $MHC\ II^+$ APCs in the viable epidermis/dermis to be observed through CLSM imaging in auricular or flank skin.[37] Microneedles were applied to ear skin for 5 min, which was then dissected 6 or 24 h later for CLSM imaging. After 6 h, we observed AF647-OVA and DiI fluorescence in clusters around microneedle insertion sites; these signals were co-localized in the same *z*-plane as epidermal APCs expressing MHC II-GFP and extended several hundred micrometers below the skin surface (Figure 4d and S3). In skin collected 24 h following treatment, we observed similar fluorescent signal co-localization (Figure 4e) at microneedle insertion sites. However, after 24 h, low- and high-magnification CLSM imaging revealed the emergence of punctate

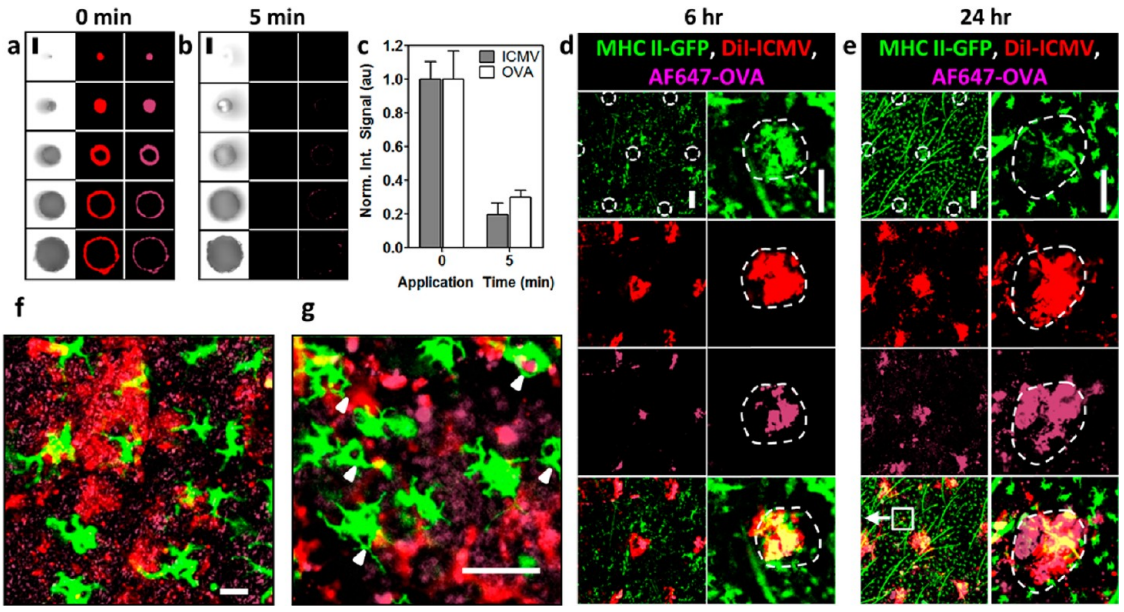

Figure 4. (a, b) Representative confocal images of PLGA microneedles coated with $(PS/SPS)_{20}(Poly\text{-}1/ICMV)_{35}$ films before application (a) and after a 5 min application to murine skin *in vivo* (b) (lateral sections, 100 μm *z*-interval; scale bar 100 μm; red, DiI-ICMVs; pink, AF647-OVA). (c) Quantitation of confocal fluorescence intensities (n = 15) showing loss of DiI-ICMV and AF647-OVA films from coated microneedles upon application to skin. (d–g) Representative confocal images of mouse skin treated for 5 min with $(PS/SPS)_{20}(Poly\text{-}1/ICMV)_{35}$ multilayer-coated PLGA microneedles after (d) 6 h or (e) 24 h showing ICMV delivery at microneedle insertion sites (outlined). Shown is fluorescent signal from (top to bottom) MHC II-GFP (green), DiI-ICMVs (red), AF647-OVA (pink), and overlay (yellow) at low (left) and high (right) magnification (scale bars 100 μm). (f) High-magnification CLSM image (field location highlighted by box in panel (e)) showing co-localization of ICMVs and OVA with APCs in the skin (scale bar 20 μm). (g) High-magnification CLSM image showing APC phagocytosis of ICMVs with OVA after 24 h (scale bar 20 μm).

fluorescent signal dispersed throughout the tissue, similar to that observed for multilayer-embedded ICMVs, suggesting multilayer disintegration and release/diffusion of ICMVs *in situ* (Figure 4e, f). This finding is consistent with the known degradation kinetics of Poly-1 multilayers, which undergo complete breakdown within 24 h.[15,38] Dispersed particles were consistently localized within the viable epidermal layers, as evidenced by co-localization within the same *z*-plane as MHC II-GFP^+ APCs (likely Langerhans cells). Further imaging indicated direct interaction between epidermal APCs and ICMVs within the treated skin, as GFP^+ cells were observed with internal fluorescent signal from both AF647-OVA and DiI (Figure 4f). In some cases, MHC II-GFP^+ APCs were observed with membrane extensions around punctate fluorescent particles, suggesting that ICMVs released from implanted multilayers were actively being phagocytosed by resident immune cells in the skin (Figure 4g).

The presence of TLR-3 and TLR-4 molecular adjuvants triggered striking changes in the APC populations present in the skin of mice with implanted ICMV multilayers (Figure 5). To determine the effect of co-delivery of ICMVs with MPLA and polyI:C, mice were treated with either uncoated microneedles or microneedle arrays delivering ICMVs with or without MPLA and polyI:C. A representative series of CLSM images from the 6 and 24 h time points following treatment were analyzed using ImageJ software particle analysis algorithms[39] to determine various phenotypically significant parameters including total cell number per field, individual cell area and perimeter, and individual cell MHC II-GFP mean fluorescent intensity (MFI). From representative CLSM fields (Figure 5a, b), as well as the dependent quantitative analysis, we observed a dramatic increase in MHC II^+ cells present in the skin tissue between 6 and 24 h for mice treated with polyI:C and microneedles coated with ICMVs encapsulating OVA with MPLA, compared to microneedles alone or microneedles coated with only ICMVs (Figure 5c). This recruitment of APCs to the microneedle application site contrasts with recent studies using microneedle arrays composed of shorter (100 μm in length) silicon needles (either bare or coated with antigens and saponin adjuvants), where a slight decrease in the density of MHC II^+ cells was observed by 24 h, suggesting activation and migration of dendritic cells toward lymphatics following patch application.[40,41] However, APC accumulation is consistent with the normal physiological response to inflammation following vaccination, as local chemokine release from stimulated keratinocytes and innate immune cells triggers both resident cell division and homing of blood-borne APCs to the inflamed tissue microenvironment.[22–24] Notably, prior studies using adjuvants such as the TLR agonist imiquimod[42] or cytokines such as GM-CSF or FLT-3 L[43,44] have shown similar infiltration of dendritic cells to skin vaccination sites (including in human

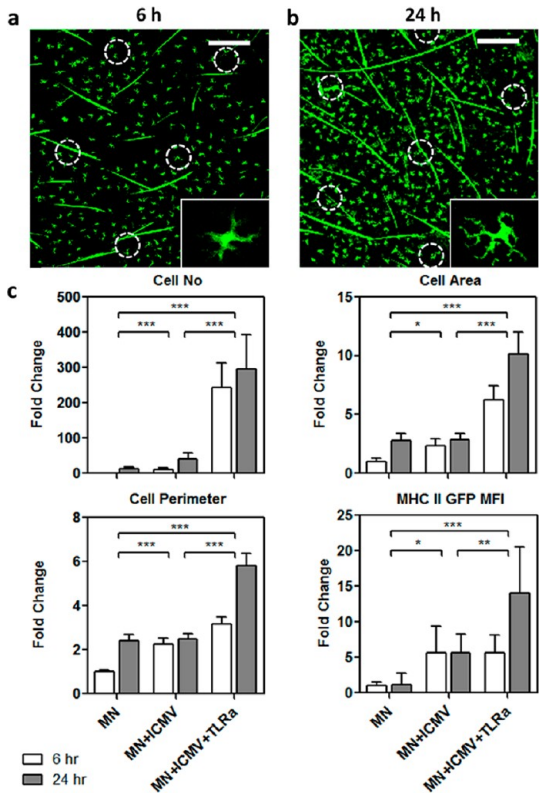

Figure 5. Representative CLSM images of MHC II-GFP$^+$ cells in skin dissected (a) 6 or (b) 24 h after $(PS/SPS)_{20}$(Poly-1/ICMV)$_{35}$-coated microneedle treatment for 5 min (insertion points outlined); ICMVs were loaded with MPLA, and polyI:C was added to the skin directly before treatment (scale bar 200 μm). (c) Results of quantitative CLSM image analysis to determine total cell number per field, individual cell area and perimeter, and MHC II-GFP MFI, expressed as fold change relative to uncoated microneedle-treated mice. Mice were treated with either uncoated microneedles (MN) or microneedles coated with $(PS/SPS)_{20}$(Poly-1/ICMV-)$_{35}$ multilayers with or without added MPLA and polyI:C (MN+ICMV and MN+ICMV+TLRa, respectively). Data were analyzed for significance using two-way ANOVA (*p < 0.05, **p < 0.01, ***p < 0.001).

trials), which correlates with greater frequencies of antigen-carrying APCs arriving at draining lymph nodes. Such dramatic APC recruitment to the application site was not observed for bare microneedles, suggesting that the response observed in this study *versus* the silicon microneedle studies cited above is not simply due to greater wounding of the skin by the larger microneedles used here.

In addition, TLR agonists trigger activation of APCs, which is accompanied by morphological changes and upregulation of MHC expression,[45−47] which we also saw reflected in skin treated with ICMVs with MPLA and polyI:C. Here individual GFP$^+$ APCs were observed to take on an extended dendritic morphology (Figure 5a, b) and increase in area (~3×), perimeter (~2×), and mean MHC II-GFP fluorescence intensity (~10×, Figure 5c) as compared with bare microneedle or ICMV-only treatments. Together these parameters are indicative of a shift toward an activated phenotype in APCs, as stimulated dendritic cells increase cellular processes to more effectively capture antigen and increase expression of MHC II for effective communication with naive lymphocytes in the generation of adaptive immunity. Thus, we have observed the effective delivery of ICMV-containing multilayers from microneedle arrays into treated skin and the subsequent disintegration of multilayer depots releasing ICMVs, which are dispersed throughout the skin for uptake by resident APCs, ultimately resulting in coincident antigen delivery and activation and maturation of the resident APC population.

Finally, we tested whether transcutaneous administration of microneedle-based multilayers encapsulating ICMVs could elicit immune responses against an antigen incorporated within ICMVs. Groups of C57Bl/6 mice were immunized on day zero and given booster immunizations after 4 weeks and 8 weeks with 1 μg of OVA (model antigen), 0.03 μg of MPLA, and 10 μg of polyI:C. For each immunization, mice received transcutaneous administration of microneedles delivering Poly-1 multilayers encapsulating either ICMVs (containing OVA and MPLA, OVA-ICMV-MN) or equivalent doses of soluble OVA (OVA-MN, Figure 6a). In both cases microneedle multilayer delivery was performed in the presence of soluble polyI:C (and MPLA in the case of OVA multilayers) applied to the skin surface before treatment. Multilayers loaded with soluble OVA were constructed on the basis of previously reported methods adapted for microneedle deposition.[27] Characterization of OVA-multilayer loading and delivery *in vivo* demonstrated effective OVA loading into microneedle-based multilayers and efficient transcutaneous delivery upon microneedle application (Figure S4). To further delineate the efficacy of microneedle-based transcutaneous vaccination from conventional bolus injection of immunogens, we also vaccinated control groups of mice by intradermal injection of ICMVs (containing OVA and MPLA, OVA-ICMV-ID) with polyI:C or soluble formulations delivering the same doses of antigen and adjuvants as in the microneedle-treated groups (OVA-ID, Figure 6a). All groups received the same total dose of OVA, MPLA, and polyI:C. Notably, following the first booster immunization all groups responded with increased OVA-specific serum IgG titers, and the total IgG titer of ICMV vaccines was identical for injected *versus* microneedle formulations by day 56 (Figure 6b). However, only mice immunized with microneedle delivery of ICMV-carrying multilayers responded to the second boost at day 56, with serum IgG titers showing an additional >10-fold increase for this group, while the other immunization regimens elicited stable or declining titers at subsequent time points. The need for multiple vaccinations to achieve this high titer is offset by the potential for enhanced protection by such a substantial increase in strength of the humoral response and the self-administrable

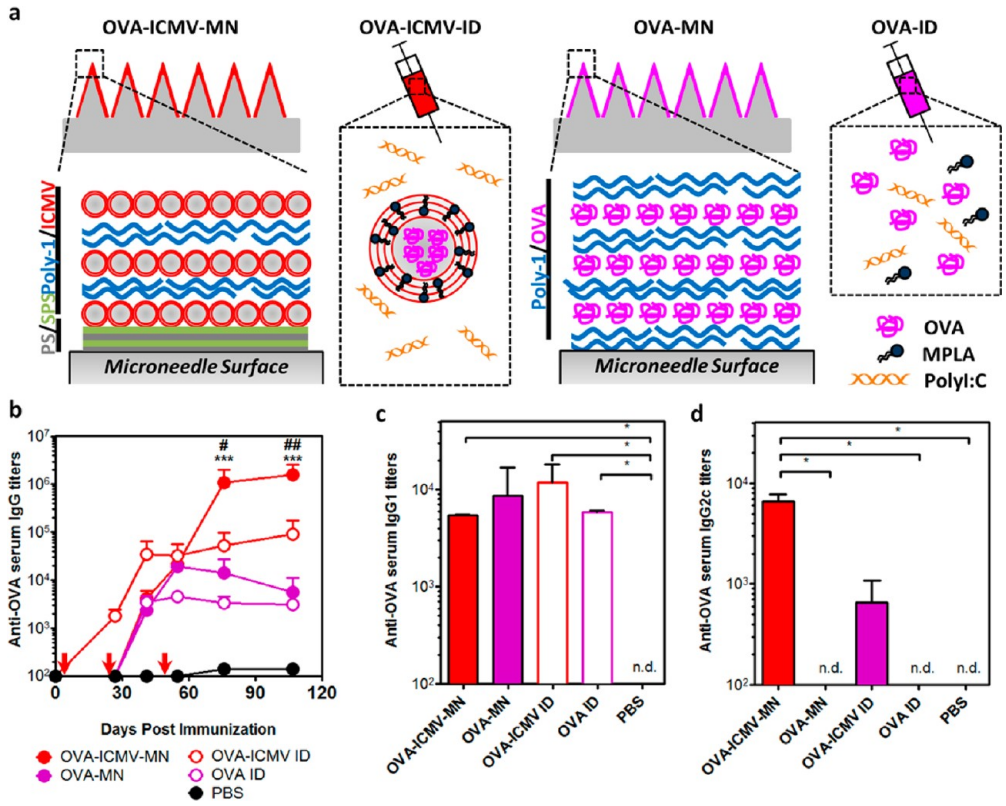

Figure 6. (a) Schematic representation of vaccine treatments tested. (b) Anti-OVA serum IgG titers were measured over time with immunizations on days 0, 28, and 56 with OVA-ICMVs or soluble antigen administered *via* either microneedle-based multilayers or intradermal bolus injection at dorsal auricular skin. (c, d) Quantification of anti-OVA IgG_1 (b) and IgG_{2c} (c) subtypes in sera at day 107. $^{\#}p < 0.05$ and $^{\#\#}p < 0.01$, compared to OVA-ICMV ID, and $^{***}p < 0.001$, compared to OVA-MN or OVA ID, as analyzed by two-way ANOVA, followed by Tukey's HSD. $^{*}p < 0.05$, as analyzed by one-way ANOVA, followed by Tukey's HSD.

nature of microneedle patch vaccines. We further analyzed sera obtained on day ~110 postimmunization to determine the isotypes of antibodies generated by transcutaneous *versus* intradermal administration of either soluble or ICMV vaccine formulations. Vaccination with free OVA protein *via* either microneedles or intradermal injection resulted in Th2-biased IgG_1 responses without any detectable level of Th1-associated IgG_{2c} antibodies (Figure 6c, d). In contrast, ICMVs administered by traditional syringe intradermally or delivered by multilayer-coated microneedles elicited a more balanced Th1/Th2 response with both IgG_1 and IgG_{2c} titers, with transcutaneous delivery of ICMV-carrying microneedles achieving 10-fold higher IgG_{2c} titers than "free" ICMV injection (Figure 6c, d). This is of interest since IgG_2 antibody isotypes have been implicated in enhanced protection in both infectious disease and cancer vaccines.[48−50] Thus, these results suggest that microneedle-based multilayers encapsulating ICMVs are a promising platform for delivery of vaccine antigen and adjuvant to skin-resident APCs *via* a noninvasive, needle-free route for promotion of long-lived, high-titer humoral immune responses.

CONCLUSIONS

In summary, we have shown the successful incorporation of intact multilamellar phospholipid vesicles into erodible multilayer films through the use of an interbilayer molecular cross-linking stabilization strategy. We have further demonstrated the potential utility of such functional multilayer coatings constructed on microneedle arrays for rapid transfer of particle-carrying multilayers into microneedle-treated skin and for the subsequent release of vesicle cargos through multilayer degradation *in situ*. Thus, this platform may ultimately serve as a potent platform for protein vaccination providing enhanced immunogenicity, simple and safe administration, and the potential for dry-state storage. These advantages provide the opportunity for more effective and less costly vaccine storage and distribution to the developing world, as multilayer stabilized formulations could be stored easily without refrigeration until rehydration upon microneedle insertion into the target tissue. Though we employed a LbL dipping process in multilayer fabrication for these lab-scale studies for convenience, note that commercial-scale processes could readily employ spray deposition to eliminate loss of precious vaccine materials during fabrication.[51] The combination of multilayer

deposition with microneedle application for transcutaneous delivery also addresses the need for a safe, potent, and noninvasive alternative to hypodermic needle-based administration. The simplicity of microneedle application also provides the prospect of rapid self-administration, potentially streamlining mass vaccination and eliminating the need for healthc are worker training.[34,52,53] In addition, the ability of ICMVs and multilayers to incorporate diverse drug compounds and biologics makes this approach of broader interest for enhanced transcutaneous delivery of therapeutics.

METHODS

Materials. Poly-1 (16 kDa) was synthesized according to previous literature.[26] Alexa Fluor 647-conjugated ovalbumin and 1,1′-dilinoleyl-3,3,3′,3′-tetramethylindocarbocyanine (DiI) were purchased from Invitrogen (Eugene, OR, USA). PLGA (50:50, IV 1.9 dL/g) was purchased from Lakeshore Biomaterials (Birmingham, AL, USA). DOPC (1,2-dioleoyl-*sn*-glycero-3-phosphocholine) and MPB (1,2-dioleoyl-*sn*-glycero-3-phosphoethanolamine-*N*-[4-(*p*-maleimidophenyl) butyramide) were purchased from Avanti Polar Lipids (Alabaster, AL, USA). MPLA was purchased from Sigma Aldrich (St. Louis, MO, USA). PolyI:C was obtained from Invivogen (San Diego, CA, USA). Chromatographically purified ovalbumin, purchased from Worthington (Lakewood, NJ, USA), was processed through Detoxi-Gels (Pierce, Rockford, IL, USA) to remove any residual endotoxin.

PLGA Microneedle Fabrication. PDMS molds (Sylgard 184, Dow Corning) were fabricated by laser ablation using a Clark-MXR CPA-2010 micromachining system (VaxDesign Inc.). PLGA pellets (IV 0.35 dL/g) were melted over the molds under vacuum (−25 in. Hg) at 140 °C for 40 min and then cooled to −20 °C before separating the cast PLGA microneedles from the PDMS mold. Microneedles were characterized by SEM using a JEOL 6700F FEG-SEM.

ICMV Synthesis. Synthesis of ICMVs was performed as described previously.[11,12] Briefly, dried films of 1.26 μmol of lipids (DOPC:MPB at 1:1 mol ratio) and 2.9 μg of MPLA were rehydrated in 20 mM bis-tris propane at pH 7.0 with 325 μg of ovalbumin for 1 h with vortexing every 10 min and sonicated in alternating power cycles of 6 and 3 W in 30 s intervals for 5 min on ice (Misonix Microson XL probe tip sonicator, Farmingdale, NY, USA). DTT and Ca^{2+} were then sequentially added at final concentrations of 3 and 40 mM, respectively, and incubated for 1 h at 37 °C to form ICMVs. The particles were recovered by centrifugation, washed twice, resuspended in PBS at pH 5.0, and stored at 4 °C until usage. In some experiments, ICMVs were prepared including a lipophilic tracer, DiI, at 0.2 molar % concentration, and 325 μg of Alexa Fluor 647-conjugated OVA was used to hydrate the lipid films.

Multilayer Film Preparation. All LbL films were assembled using a Carl Ziess HMS DS50 slide stainer. Films were constructed on Si wafers and PLGA microneedle arrays. To build (PS/SPS) base layers, substrates were dipped alternatively into PS (2 mg/mL, PBS, Sigma-Aldrich) and SPS (5 mM, PBS, Sigma-Aldrich) solutions for 10 min, separated by two sequential 1 min rinses in PBS. (Poly-1/ICMV) and (Poly-1/MLV) multilayers were deposited similarly, alternating 5 min dips in Poly-1 (2 mg/mL, PBS) and ICMV/MLV solutions (1 mg/mL, PBS) separated by two sequential 30 s rinsing steps in PBS. (Poly-1/OVA) multilayers were deposited by alternating 10 min dips in Poly-1 (2 mg/mL, 0.2 M sodium acetate) and OVA solutions (0.1 mg/mL, 0.2 M sodium acetate) separated by two sequential 1 min rinsing steps in deionized water. All solutions were adjusted to pH 5.0 and filtered (0.2 μm, except ICMV/MLV and OVA) prior to dipping.

Multilayer Film Characterization. Film thickness on Si wafers was characterized using a Veeco Dektak (Plainview, NY, USA) surface profilometer and a Veeco Dimension 3100 AFM. Film growth and morphology on PLGA microneedles were characterized by SEM using a JEOL 6700F FEG-SEM and CLSM using a Carl Zeiss LSM 510. Data analysis was performed using ImageJ[39] and Graphpad Prism (La Jolla, CA, USA). Film loading was determined for fluorescent cargos using a SpectraMax 250 spectrophotometer (Molecular Devices, Sunnyvale, CA, USA) following elution of films in PBS, pH 7.4, 2 M NaCl for 24 h.

Characterization of Film Delivery *in Vivo*. ICMV or soluble OVA delivery was measured *in vivo* following application of coated microneedles to the skin of mice. Animals were cared for in the USDA-inspected MIT Animal Facility under federal, state, local, and NIH guidelines for animal care. Microneedle application experiments were performed on anesthetized 6−10-week-old female C57BL/6 (Jackson Laboratories) and C57Bl/6-MHC II-GFP transgenic mice (a gift from Prof. Hidde Ploegh, MIT) at the dorsal ear or flank skin. Skin was rinsed briefly with PBS and dried before application of microneedle arrays by gentle pressure. Following application, mice were euthanized at subsequent time points, and the application site was dissected. Excised skin was stained with trypan blue before imaging for needle penetration. In separate experiments treated skin and applied microneedle arrays were imaged by confocal microscopy to assess transcutaneous delivery of encapsulated ICMVs or soluble OVA. MHC II-GFP^+ cell number and morphology were analyzed by CLSM in dissected tissue following microneedle treatment. Image analysis was performed using NIH ImageJ software.[39]

Vaccinations and Characterization of Humoral Immune Responses. Groups of 6−10-wk-old female C57Bl/6 mice were immunized on days 0, 28, and 56 with 1 μg of OVA, 0.03 μg of MPLA, and 10 μg of polyI:C in either suspension or microneedle formulations. Microneedle coating compositions were chosen so that the dose of antigen/MPLA delivered into the skin matched the injected cases: microneedle coatings were dissolved in sodium chloride buffer, and the amount of antigen present was assessed using a spectrofluorimeter for as-prepared and postskin-application microneedles; the delivered dose was determined as the difference between these two values. For intradermal administration, immunogens in 15 μL of PBS were injected intradermally in the dorsal auricular skin. Transcutaneous administration of microneedles was performed as described above, following brief rinsing with sterile PBS at the dorsal ear skin. For multilayers containing OVA/MPLA-loaded ICMVs, polyI:C was administered in 5 μL of PBS to the surface of the skin prior to treatment and left in place during the duration of microneedle application. For multilayers containing soluble OVA, polyI:C and MPLA were similarly administered to the skin prior to microneedle treatment. Microneedles were secured in place for 5 min for both ICMV- and soluble OVA-containing multilayer coating variations. Sera obtained from immunized mice at various time points were analyzed for IgG, IgG_1, and IgG_{2c} antibodies by ELISA using OVA-coated plates. Anti-OVA IgG titers were defined as the lowest serum dilution at which the ELISA OD reading was $\geq$0.5.

Statistical Analysis. Data sets were analyzed using one- or two-way analysis of variance (ANOVA), followed by Tukey's HSD test for multiple comparisons with Prism 5.0 (GraphPad Software, San Diego, CA, USA). *p*-Values less than 0.05 were considered statistically significant. All values are reported as mean ± SEM.

Conflict of Interest: The authors declare no competing financial interest.

Acknowledgment. This work was supported in part by the Ragon Institute of MGH, MIT, and Harvard, the NIH (AI095109), the MIT Institute for Soldier Nanotechnology, Army Research Office, and the Dept. of Defense (W911NF-07-D-0004 and W911NF-07-D-0004, T.O. 8). D.J.I. is an investigator of the Howard Hughes Medical Institute.

Supporting Information Available: Chemical structures of reagents, additional AFM and CLSM analysis, and characterization

of multilayers containing soluble ovalbumin. This material is available free of charge *via* the Internet at http://pubs.acs.org.

REFERENCES AND NOTES

1. DeVilliers, M. M.; Otto, D. P.; Strydom, S. J.; Lvov, Y. M. Introduction to Nanocoatings Produced by Layer-by-Layer (LbL) Self-Assembly. *Adv. Drug Delivery Rev.* **2011**, *63*, 701–715.
2. Hammond, P. T. Engineering Materials Layer-by-Layer: Challenges and Apportunities in Multilayer Assembly. *AIChE J.* **2011**, *57*, 2928–2940.
3. Katagiri, K.; Hamasaki, R.; Ariga, K.; Kikuchi, J.-i. Layered Paving of Vesicular Nanoparticles Formed with Cerasome as a Bioinspired Organic-Inorganic Hybrid. *J. Am. Chem. Soc.* **2002**, *124*, 7892–7893.
4. Katagiri, K.; Hamasaki, R.; Ariga, K.; Kikuchi, J.-i. Layer-by-Layer Self-Assembling of Liposomal Nanohybrid "Cerasome" on Substrates. *Langmuir* **2002**, *18*, 6709–6711.
5. Graf, N.; Tanno, A.; Dochter, A.; Rothfuchs, N.; Voeroes, J.; Zambelli, T. Electrochemically Driven Delivery to Cells from Vesicles Embedded in Polyelectrolyte Multilayers. *Soft Matter* **2012**, *8*, 3641–3648.
6. Michel, M.; Arntz, Y.; Fleith, G.; Toquant, J.; Haikel, Y.; Voegel, J.-C.; Schaaf, P.; Ball, V. Layer-by-Layer Self-Assembled Polyelectrolyte Multilayers with Embedded Liposomes: Immobilized Submicronic Reactors for Mineralization. *Langmuir* **2006**, *22*, 2358–2364.
7. Michel, M.; Izquierdo, A.; Decher, G.; Voegel, J. C.; Schaaf, P.; Ball, V. Layer by Layer Self-Assembled Polyelectrolyte Multilayers with Embedded Phospholipid Vesicles Obtained by Spraying: Integrity of the Vesicles. *Langmuir* **2005**, *21*, 7854–7859.
8. Michel, M.; Vautier, D.; Voegel, J.-C.; Schaaf, P.; Ball, V. Layer by Layer Self-Assembled Polyelectrolyte Multilayers with Embedded Phospholipid Vesicles. *Langmuir* **2004**, *20*, 4835–4839.
9. Volodkin, D.; Arntz, Y.; Schaaf, P.; Moehwald, H.; Voegel, J.-C.; Ball, V. Composite Multilayered Biocompatible Polyelectrolyte Films with Intact Liposomes: Stability and Temperature Triggered Dye Release. *Soft Matter* **2008**, *4*, 122–130.
10. Volodkin, D. V.; Schaaf, P.; Mohwald, H.; Voegel, J.-C.; Ball, V. Effective Embedding of Liposomes into Polyelectrolyte Multilayered Films: the Relative Importance of Lipid-Polyelectrolyte and Interpolyelectrolyte Interactions. *Soft Matter* **2009**, *5*, 1394–1405.
11. Moon, J. J.; Suh, H.; Bershteyn, A.; Stephan, M. T.; Liu, H.; Huang, B.; Sohail, M.; Luo, S.; Um, S. H.; Khant, H.; *et al.* Interbilayer-Crosslinked Multilamellar Vesicles as Synthetic Vaccines for Potent Humoral and Cellular Immune Responses. *Nat. Mater.* **2011**, *10*, 243–251.
12. Moon, J. J.; Suh, H.; Li, A. V.; Ockenhouse, C. F.; Yadava, A.; Irvine, D. J. Enhancing Humoral Responses to a Malaria Antigen with Nanoparticle Vaccines that Expand Tfh Cells and Promote Germinal Center Induction. *Proc. Natl. Acad. Sci. U. S. A.* **2012**, *109*, 1080–1085.
13. Wermeling, D. P.; Banks, S. L.; Hudson, D. A.; Gill, H. S.; Gupta, J.; Prausnitz, M. R.; Stichcomb, A. L. Microneedles Permit Transdermal Delivery of a Skin-Impermeant Medication to Humans. *Proc. Natl. Acad. Sci. U. S. A.* **2008**, *105*, 2058–2063.
14. Zhu, Q.; Zarnitsyn, V. G.; Ye, L.; Wen, Z.; Gao, Y.; Pan, L.; Skountzou, I.; Gill, H. S.; Prausnitz, M. R.; Yang, C.; *et al.* Immunization by Vaccine-Coated Microneedle Arrays Protects Against Lethal Influenza Virus Challenge. *Proc. Natl. Acad. Sci. U. S. A.* **2009**, *106*, 7968–7973.
15. DeMuth, P. C.; Su, X.; Samuel, R. E.; Hammond, P. T.; Irvine, D. J. Nano-layered Microneedles for Transcutaneous Delivery of Polymer Nanoparticles and Plasmid DNA. *Adv. Mater.* **2010**, *22*, 4851–4856.
16. Chen, X.; Kask, A. S.; Crichton, M. L.; McNeilly, C.; Yukiko, S.; Dong, L.; Marshak, J. O.; Jarrahian, C.; Fernando, G. J. P.; Chen, D.; *et al.* Improved DNA Vaccination by Skin-Targeted Delivery Using Dry-Coated Densely-Packed Microprojection Arrays. *J. Controlled Release* **2010**, *148*, 327–333.
17. Sullivan, S. P.; Koutsonanos, D. G.; Del Pilar, M. M.; Lee Jeong, W.; Zarnitsyn, V.; Choi Seong, O.; Murthy, N.; Compans, R. W.; Skountzou, I.; Prausnitz, M. R. Dissolving Polymer Microneedle Patches for Influenza Vaccination. *Nat. Med.* **2009**, *16*, 915–20.
18. Donatus, U.; Bruce, G.; Robert, T. Model-Based Estimates of Risks of Disease Transmission and Economic Costs of Seven Injection Devices in Sub-Saharan Africa. *Bull. W. H. O.* **2002**, *80*, 859–70.
19. Pruss-Ustun, A.; Rapita, E.; Hutin, Y., *Sharps Injuries: Global Burden of Disease from Sharps Injuries to Health-Care Workers*; World Health Organization, 2003.
20. Giudice, E. L.; Campbell, J. D. Needle-Free Vaccine Delivery. *Adv. Drug Delivery Rev.* **2006**, *58*, 68–89.
21. Saurer, E. M.; Flessner, R. M.; Sullivan, S. P.; Prausnitz, M. R.; Lynn, D. M. Layer-by-Layer Assembly of DNA- and Protein-Containing Films on Microneedles for Drug Delivery to the Skin. *Biomacromolecules* **2010**, *11*, 3136–3143.
22. Kupper, T. S.; Fuhlbrigge, R. C. Immune Surveillance in the Skin: Mechanisms and Clinical Consequences. *Nat. Rev. Immunol.* **2004**, *4*, 211–222.
23. Merad, M.; Ginhoux, F.; Collin, M. Origin, Homeostasis and Function of Langerhans Cells and Other Langerin-Expressing Dendritic Cells. *Nat. Rev. Immunol.* **2008**, *8*, 935–947.
24. Nestle, F. O.; Di Meglio, P.; Qin, J.-Z.; Nickoloff, B. J. Skin Immune Sentinels in Health and Disease. *Nat. Rev. Immunol.* **2009**, *9*, 679–691.
25. Jewell, C. M.; Lynn, D. M. Multilayered Polyelectrolyte Assemblies as Platforms for the Delivery of DNA and Other Nucleic Acid-Based Therapeutics. *Adv. Drug Delivery Rev.* **2008**, *60*, 979–999.
26. Lynn, D. M.; Langer, R. Degradable Poly(Beta-amino esters): Synthesis, Characterization, and Self-Assembly with Plasmid DNA. *J. Am. Chem. Soc.* **2000**, *122*, 10761–10768.
27. Su, X.; Kim, B.-S.; Kim Sara, R.; Hammond Paula, T.; Irvine Darrell, J. Layer-by-Layer-Assembled Multilayer Films for Transcutaneous Drug and Vaccine Delivery. *ACS Nano* **2009**, *3*, 3719–29.
28. Akinc, A.; Anderson, D. G.; Lynn, D. M.; Langer, R. Synthesis of Poly(Beta-Amino Ester)s Optimized for Highly Effective Gene Delivery. *Bioconjugate Chem.* **2003**, *14*, 979–988.
29. Greenland, J. R.; Liu, H.; Berry, D.; Anderson, D. G.; Kim, W.-K.; Irvine, D. J.; Langer, R.; Letvin, N. L. Beta-Amino Ester Polymers Facilitate in Vivo DNA Transfection and Adjuvant Plasmid DNA Immunization. *Mol. Ther.* **2005**, *12*, 164–170.
30. Samuel, R. E.; Shukla, A.; Paik, D. H.; Wang, M. X.; Fang, J. C.; Schmidt, D. J.; Hammond, P. T. Osteoconductive Protamine-Based Polyelectrolyte Multilayer Functionalized Surfaces. *Biomaterials* **2011**, *32*, 7491–7502.
31. Ichinose, I.; Fujiyoshi, K.; Mizuki, S.; Lvov, Y.; Kunitake, T. Layer-by-Layer Assembly of Aqueous Bilayer Membranes on Charged Surfaces. *Chem. Lett.* **1996**, 257–258.
32. Zhang, L.; Longo, M. L.; Stroeve, P. Mobile Phospholipid Bilayers Supported on a Polyion/Alkylthiol Layer Pair. *Langmuir* **2000**, *16*, 5093–5099.
33. Babiuk, S.; Baca-Estrada, M.; Babiuk, L. A.; Ewen, C.; Foldvari, M. Cutaneous Vaccination: the Skin as an Immunologically Active Tissue and the Challenge of Antigen Delivery. *J. Controlled Release* **2000**, *66*, 199–214.
34. Glenn, G. M.; Kenney, R. T.; Ellingsworth, L. R.; Frech, S. A.; Hammond, S. A.; Zoeteweij, J. P. Transcutaneous Immunization and Immunostimulant Strategies: Capitalizing on the Immunocompetence of the Skin. *Expert Rev. Vaccines* **2003**, *2*, 253–267.
35. Warger, T.; Schild, H.; Rechtsteiner, G. Initiation of Adaptive Immune Responses by Transcutaneous Immunization. *Immunol. Lett.* **2007**, *109*, 13–20.
36. Gill, H. S.; Prausnitz, M. R. Coating formulations for microneedles. *Pharm. Res.* **2007**, *24*, 1369–1380.
37. Boes, M.; Cerny, J.; Massol, R.; Op den Brouw, M.; Kirchhausen, T.; Chen, J.; Ploegh Hidde, L. T-cell Engagement of Dendritic Cells Rapidly Rearranges MHC Class II Transport. *Nature* **2002**, *418*, 983–8.

38. Zhang, J.; Chua, L. S.; Lynn, D. M. Multilayered Thin Films that Sustain the Release of Functional DNA under Physiological Conditions. *Langmuir* **2004**, *20*, 8015–8021.
39. Abramoff, M. D.; Magelhaes, P. J.; Ram, S. J. Image Processing with Image J. *Biophotonics International* **2004**, *11*, 36–42.
40. Prow, T. W.; Chen, X.; Prow, N. A.; Fernando, G. J. P.; Tan, C. S. E.; Raphael, A. P.; Chang, D.; Ruutu, M. P.; Jenkins, D. W. K.; Pyke, A.; *et al*. Nanopatch-Targeted Skin Vaccination against West Nile Virus and Chikungunya Virus in Mice. *Small* **2010**, *6*, 1776–1784.
41. Ruutu, M. P.; Chen, X.; Joshi, O.; Kendall, M. A.; Frazer, I. H. Increasing Mechanical Stimulus Induces Migration of Langerhans Cells and Impairs the Immune Response to Intracutaneously Delivered Antigen. *Exp. Dermatol.* **2011**, *20*, 534–536.
42. Adams, S.; O'Neill, D. W.; Nonaka, D.; Hardin, E.; Chiriboga, L.; Siu, K.; Cruz, C. M.; Angiulli, A.; Angiulli, F.; Ritter, E.; *et al*. Immunization of Malignant Melanoma Patients with Full-Length NY-ESO-1 Protein Using TLR7 Agonist Imiquimod as Vaccine Adjuvant. *J. Immunol.* **2008**, *181*, 776–784.
43. Mwangi, W.; Brown, W. C.; Lewin, H. A.; Howard, C. J.; Hope, J. C.; Baszler, T. V.; Caplazi, P.; Abbott, J.; Palmer, G. H. DNA-Encoded Fetal Liver Tyrosine Kinase 3 Ligand and Granulocyte Macrophage-Colony-Stimulating Factor Increase Dendritic Cell Recruitment to the Inoculation Site and Enhance Antigen-Specific CD4+ T Cell Responses Induced by DNA Vaccination of Outbred Animals. *J. Immunol.* **2002**, *169*, 3837–3846.
44. Soiffer, R.; Lynch, T.; Mihm, M.; Jung, K.; Rhuda, C.; Schmollinger, J. C.; Hodi, F. S.; Liebster, L.; Lam, P.; Mentzer, S.; *et al*. Vaccination with Irradiated Autologous Melanoma Cells Engineered to Secrete Human Granulocyte-Macrophage Colony-Stimulating Factor Generates Potent Antitumor Immunity in Patients with Metastatic Melanoma. *Proc. Natl. Acad. Sci. U. S. A.* **1998**, *95*, 13141–13146.
45. Akira, S.; Uematsu, S.; Takeuchi, O. Pathogen Recognition and Innate Immunity. *Cell* **2006**, *124*, 783–801.
46. Gay, N. J.; Gangloff, M.; Weber, A. N. R. Toll-Like Receptors as Molecular Switches. *Nat. Rev. Immunol.* **2006**, *6*, 693–698.
47. Manicassamy, S.; Pulendran, B. Modulation of Adaptive Immunity with Toll-Like Receptors. *Semin. Immunol.* **2009**, *21*, 185–193.
48. Aucan, C.; Traore, Y.; Tall, F.; Nacro, B.; Traore-Leroux, T.; Fumoux, F.; Rihet, P. High Immunoglobulin G2 (IgG2) and Low IgG4 Levels are Associated with Human Resistance to Plasmodium Falciparum Malaria. *Infect. Immun.* **2000**, *68*, 1252–1258.
49. Beenhouwer, D. O.; Yoo, E. M.; Lai, C.-W.; Rocha, M. A.; Morrison, S. L. Human Immunoglobulin G2 (IgG2) and IgG4, but Not IgG1 or IgG3, Protect Mice Against Cryptococcus Neoformans Infection. *Infect. Immun.* **2007**, *75*, 1424–1435.
50. Nimmerjahn, F.; Ravetch, J. V. Divergent Immunoglobulin G Subclass Activity Through Selective Fc Receptor Binding. *Science* **2005**, *310*, 1510–1512.
51. Krogman, K. C.; Lowery, J. L.; Zacharia, N. S.; Rutledge, G. C.; Hammond, P. T. Spraying Asymmetry into Functional Membranes Layer-by-Layer. *Nat. Mater.* **2009**, *8*, 512–518.
52. Kim, Y.-C.; Quan, F.-S.; Yoo, D.-G.; Compans Richard, W.; Kang, S.-M.; Prausnitz Mark, R. Enhanced Memory Responses to Seasonal H1N1 Influenza Vaccination of the Skin with the Use of Vaccine-Coated Microneedles. *J. Infect. Dis.* **2010**, *201*, 190–198.
53. Quan, F.-S.; Kim, Y.-C.; Yoo, D.-G.; Compans, R. W.; Prausnitz, M. R.; Kang, S.-M. Stabilization of Influenza Vaccine Enhances Protection by Microneedle Delivery in the Mouse Skin. *PLoS One* **2009**, *4*, e7152.